

OPTIMAL DESIGN IN VIBRO-ACOUSTIC PROBLEMS INVOLVING PERFORATED PLATES

Eduard Rohan, Vladimír Lukeš

Department of Mechanics, Faculty of Applied Sciences, University of West Bohemia, Univerzitní 8,
30614 Pilsen, Czech Republic,
rohan@kme.zcu.cz

Keywords: Vibroacoustics, Homogenization, Perforated Plate, Sensitivity Analysis, Optimization, Acoustic Transmission.

Abstract. *The paper deals with design sensitivity and optimization of perforated plates which interact with acoustic waves. Transmission conditions for coupling the acoustic pressure fields on both sides of the interface were derived using the homogenization of vibroacoustic interactions in a fictitious layer in which the Reissner-Mindlin type of deforming plate is embedded. The sensitivity analysis of an objective function with respect to the perforation design is based on the shape derivatives and the adjoint equation technique. The problem of minimization, or maximization of transmission losses in a waveguide containing the plate can be solved to find piecewise periodic design of the plate perforation the shape of which is described with a few optimization parameters.*

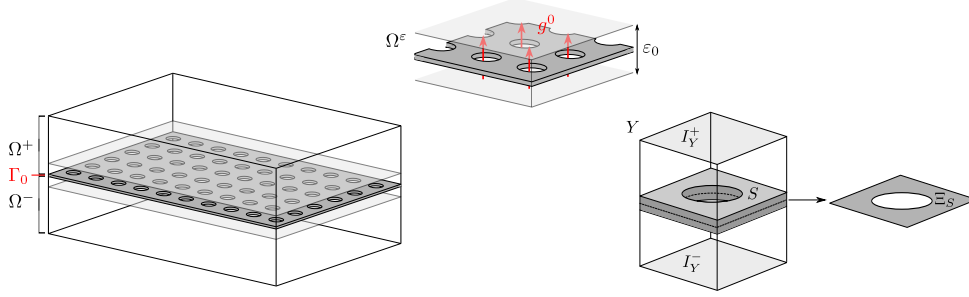


Figure 1: Left: The global domain decomposition into Ω^+ and Ω^- separated by the homogenized perforated plate represented on the interface Γ_0 . Center: The transmission conditions were derived using homogenization of the vibroacoustic problem, the acoustic pressure jump is proportional to the transverse acoustic velocity g^0 . Right: perforated interface and the representative periodic cell $Y = Y^* \cup \bar{S}$.

1 INTRODUCTION

We consider problems of the acoustic wave propagation through vibrating perforated plates. The aim is to reduce the noise produced by a source, transmitted through the acoustic fluid and influenced by perforated compliant plates. There are many challenging applications of this problem in the aerospace and automotive engineering.

The acoustic problem described by the Helmholtz equation involves homogenized transmission conditions imposed along a compliant plate. In [6], using the asymptotic analysis we developed the homogenized transmission conditions to be imposed on the interface plane representing the slab with a periodic perforation which, in general, is designed by obstacles having arbitrarily complicated shapes. The compliant plates were treated in [8], cf. [9] where the framework of the Reissner-Mindlin theory was used to derive the vibro-acoustic transmission conditions which take into account specific shapes of the holes in the plate.

The design variables modify locally the shape of the perforation, i.e. for any “macroscopic” point on the homogenized plate interface, a special set of design variables can be considered. Some smoothness constraints are involved in the formulation; this is necessary for eligibility of the homogenization method. The state problem and, thereby, also the sensitivity analysis comprise two levels, see Section 2: a) the macroscopic problem involving the homogenized transmission coefficients (HTC), b) the local microscopic problems solved in computational cells; the local solutions define the HTCs.

In Section 3, we present the sensitivity analysis based on the adjoint system technique. Numerical examples of optimization problems and computing the sensitivities of the transmission loss with respect to the HTC depending on the shape of the perforation coefficients involved in the vibro-acoustic transmission model are presented in Section 4.

We consider the global problem of the wave propagation in a duct $\Omega^G \subset \mathbb{R}^3$ filled by the acoustic fluid. Ω^G is subdivided by perforated plate Γ_0 in two disjoint subdomains Ω^+ and Ω^- , so that $\Omega^G = \Omega^+ \cup \Omega^- \cup \Gamma_0$, see Figure 1. The acoustic pressure field p is discontinuous in general along Γ_0 . In a case of no convection flow (the linear acoustics), the waves propagating in Ω are described by the following equations where ω is the wave frequency (i.e. $\omega = \kappa c$ where c is the sound speed and κ is the wave number)

$$\begin{aligned}
 c^2 \nabla^2 p + \omega^2 p &= 0 \quad \text{in } \Omega^+ \cup \Omega^-, \\
 \text{transmission conditions } \mathcal{G}(\omega, [p]_-, [\partial p / \partial n]_+) &= 0 \quad \text{on } \Gamma_0, \\
 ri\omega p + c^2 \frac{\partial p}{\partial n} &= s2i\omega \bar{p} \quad \text{on } \partial\Omega,
 \end{aligned} \tag{1}$$

where s, r and \bar{p} are given data, $[\cdot]_{\pm}^{\pm}$ is the jump across Γ_0 and $\frac{\partial p}{\partial n} = \mathbf{n} \cdot \nabla p$ is the normal derivative on Γ_0 . Boundary $\partial\Omega = \Gamma_w \cup \Gamma_{\text{in}} \cup \Gamma_{\text{out}}$ of the duct is split into walls and the input/output parts; by the constants r, s in (1)₃ different conditions on $\partial\Omega$ are respected: $r = s = 0$ on the duct walls Γ_w , whereas $r = s = 1$ on Γ_{in} and $r = 1, s = 0$ on Γ_{out} .

The homogenized transmission conditions $\mathcal{G} = 0$, see (1), was developed in [6] for rigid plates and general shape of the holes; two internal variables on Γ_0 were introduced: the “in-layer” acoustic pressure p^0 and the “transversal” acoustic velocity g^0 , which is coupled with the global fields through: $c^2 \partial p / \partial n^{\pm} = \pm i \omega g^0$, so that $[\partial p / \partial n]_{\pm}^{\pm} = 0$. In [3] we reported on homogenization of the vibro-acoustic transmission on the perforated plate. Since we relied on an extension of the homogenized Reissner-Mindlin plate tailor-made for perforation by general cylindrical holes with axes orthogonal to the mid-plane of the plate, the transmission problem led to two subproblems: the membrane “in-plane” modes of the plate vibrations coupled with surface tangent acoustic waves and the deflection-rotation modes of the plate vibrations coupled with the exterior acoustic fields. In this paper we focus on the latter problem in which the transmission condition involves the transversal acoustic velocity g^0 .

2 THE STATE PROBLEM OF OPTIMIZATION INVOLVING THE HOMOGENIZED PLATE

By virtue of the homogenization method applied to derive the acoustic transmission condition, the state problem is decomposed into the *global problem* and the *local problems*, the latter being related to a specific perforation geometries for which the homogenized coefficients are computed.

2.1 The global state problem

The global vibroacoustic problem involving the homogenized plate is described in terms of the quadruple $\mathbf{U} := (p, g^0, w, \boldsymbol{\theta})$, where p is the global acoustic pressure field defined in Ω , being discontinuous on Γ_0 representing the plate, g^0 is the transversal acoustic velocity on Γ_0 , w is the plate deflection and $\boldsymbol{\theta}$ describes the rotation of the plate transversal sections (w.r.t. a rigid frame). To introduce the weak formulation, we employ the test fields $\mathbf{V} = (q, \psi, z, \boldsymbol{\vartheta})$ associated with \mathbf{U} . The following bilinear forms are introduced, where in the r.h.s. expressions $\langle \cdot, \cdot \rangle_{\Gamma_0}$ is the inner product on Γ_0 and $F, C_3, \mathbf{G}^H, \mathbf{C}^H$ and T_{33} are the homogenized coefficients defined in Section 2.2, Eq. (8), for the local perforation geometries, thus, being functions of $x \in \Gamma_0$: The inertia and fluid-structure interaction effects are associated with

$$\begin{aligned} \mathcal{F}(g, \psi) &= \langle Fg, \psi \rangle_{\Gamma_0} , \\ \mathcal{C}(u, \psi) &= \langle C_3 u, \psi \rangle_{\Gamma_0} , \\ \mathcal{N}(u, z) &= \left\langle \left(h \frac{\bar{\rho}_S}{\rho_0} + T_{33} \right) u, z \right\rangle_{\Gamma_0} , \\ \mathcal{M}(\boldsymbol{\theta}, \boldsymbol{\vartheta}) &= \frac{h^3}{3} \left\langle \frac{\bar{\rho}_S}{\rho_0} \boldsymbol{\theta}, \boldsymbol{\vartheta} \right\rangle_{\Gamma_0} . \end{aligned} \tag{2}$$

whereas the plate stiffness in shear and bending effects are associated with

$$\begin{aligned} \mathcal{G}(\bar{\nabla} w, \boldsymbol{\vartheta}) &= h \langle \mathbf{G}^H \bar{\nabla} w, \boldsymbol{\vartheta} \rangle_{\Gamma_0} , \\ \mathcal{E}(\bar{\nabla}^S \boldsymbol{\theta}, \bar{\nabla}^S \boldsymbol{\vartheta}) &= \frac{h^3}{3} \left\langle \mathbf{C}^H \bar{\nabla}^S \boldsymbol{\theta}, \bar{\nabla}^S \boldsymbol{\vartheta} \right\rangle_{\Gamma_0} , \end{aligned} \tag{3}$$

where h is the plate thickness, $\bar{\rho}_S$ is the effective plate density and ρ_0 is the fluid density.

The state problem reads, as follows: Find $\mathbf{U} := (p, g, w, \boldsymbol{\theta}) \in \mathcal{U} = H_{-1}^1(\Omega, \Gamma_0) \times L^2(\Gamma_0) \times H_0^1(\Gamma_0) \times \mathbf{H}_0^1(\Gamma_0)$, such that

$$\Psi(\mathbf{U}, \mathbf{V}) = f(\mathbf{V}) \quad \forall \mathbf{V} = (q, \psi, z, \boldsymbol{\vartheta}) \in \mathcal{U}_0 = \mathcal{U}, \quad (4)$$

where

$$\begin{aligned} \Psi(\mathbf{U}, \mathbf{V}) &:= c^2 (\nabla p, \cdot \nabla q)_\Omega - \omega^2 (p, q)_\Omega + i\omega c \langle p, q \rangle_{\Gamma_{\text{in-out}}} - i\omega c^2 \langle g, q^+ - q^- \rangle_{\Gamma_0} \\ &\quad + \omega^2 [\mathcal{C}(w, \psi) + \mathcal{C}(z, g) - \mathcal{F}(g, \psi) - \mathcal{N}(w, z) - \mathcal{M}(\boldsymbol{\theta}, \boldsymbol{\vartheta})] \\ &\quad + \mathcal{E}(\bar{\nabla}^S \boldsymbol{\theta}, \bar{\nabla}^S \boldsymbol{\vartheta}) + \mathcal{G}(\bar{\nabla} w - \boldsymbol{\theta}, \bar{\nabla} z - \boldsymbol{\vartheta}) - i\omega \frac{1}{\varepsilon_0} \langle \psi, p^+ - p^- \rangle_{\Gamma_0}, \\ f(\mathbf{V}) &:= 2i\omega \langle \bar{p}, q \rangle_{\Gamma_{\text{in}}}, \end{aligned} \quad (5)$$

and \mathcal{U} is the set of admissible solutions. In (4), by $H_{-1}^1(\Omega, \Gamma_0)$ we denote the space of piecewise weakly differentiable functions with discontinuity on Γ_0 ,

$$H_{-1}^1(\Omega, \Gamma_0) = L^2(\Omega) \cap H^1(\Omega^+ \cup \Omega^-), \quad \Gamma_0 = \overline{\Omega^+} \cap \overline{\Omega^-}.$$

2.2 The local state problems and formulae for the transmission parameters

The homogenized transmission conditions are introduced in terms of local response functions defined in the representative periodic cell $Y \subset \mathbb{R}^3$ describing the perforation geometry. Let $Y = \Xi \times]-1/2, +1/2[$, where $\Xi =]0, 1[\times]0, 1[$ is on the mid-plane of the plate. By $S \subset Y$ we denote the solid part of the cell which represents a segment of the plate immersed in the acoustic fluid occupying $Y^* = Y \setminus \bar{S}$. Only cylindrical holes “orthogonal” to the plate mid-plane can be considered, but otherwise their shape can be quite arbitrary. Thus, the solid part of the representative periodic cell is situated in $\Xi \times]-h^Y/2, +h^Y/2[$ where $h^Y \ll 1/2$ is the “relative plate thickness”. The plate segment is generated using Ξ_S defined in terms of the “hole shape” Γ_S , see Fig. 2, so that $\Xi = \Xi_S \times]-h^Y/2, +h^Y/2[$ is a cylinder. The geometry just introduced will be called the “simple perforation design”.

Below we use the space $H_{\#(\Xi)}^1(Y^*)$ constituted by all Ξ -periodic functions in the Sobolev space $H^1(Y^*)$ (as the consequence, $H_{\#(\Xi_S)}^1(\Xi_S)$ is constituted by all Ξ -periodic functions). Functions $\xi, \eta^k \in H_{\#(\Xi)}^1(Y^*)$ satisfy ($I_y^\pm = \{y \in \partial \bar{Y} \mid y_3 = \pm 1/2\}$)

$$\begin{aligned} (\nabla_y \xi, \nabla_y \psi)_{Y^*} &= - \left(\int_{I_y^+} \psi - \int_{I_y^-} \psi \right), \\ (\nabla_y \eta^k, \nabla_y \psi)_{Y^*} &= - \int_{\partial S} n_k \psi, \quad k = 1, 2, 3, \end{aligned} \quad (6)$$

for all $\psi \in H_{\#(\Xi)}^1(Y^*)$. Functions $\bar{\chi}^{rs} \in \mathbf{H}_{\#(\Xi_S)}^1(\Xi_S)/\mathbb{R}$ and $\chi^k \in H_{\#(\Xi_S)}^1(\Xi_S)/\mathbb{R}$, $k, r, s = 1, 2$, satisfy

$$\begin{aligned} \int_{\Xi_S} (\mathbf{C} \bar{\nabla}_y^S (\bar{\chi}^{rs} + \boldsymbol{\Pi}^{rs}) : \bar{\nabla}_y^S \bar{\mathbf{v}} &= 0 \quad \forall \bar{\mathbf{v}} \in \mathbf{H}_{\#(\Xi_S)}^1(\Xi_S), \\ \int_{\Xi_S} \gamma \nabla_y (\chi^k + y_k) \cdot \nabla_y \tilde{z} &= 0 \quad \forall \tilde{z} \in H_{\#(\Xi_S)}^1(\Xi_S), \end{aligned} \quad (7)$$

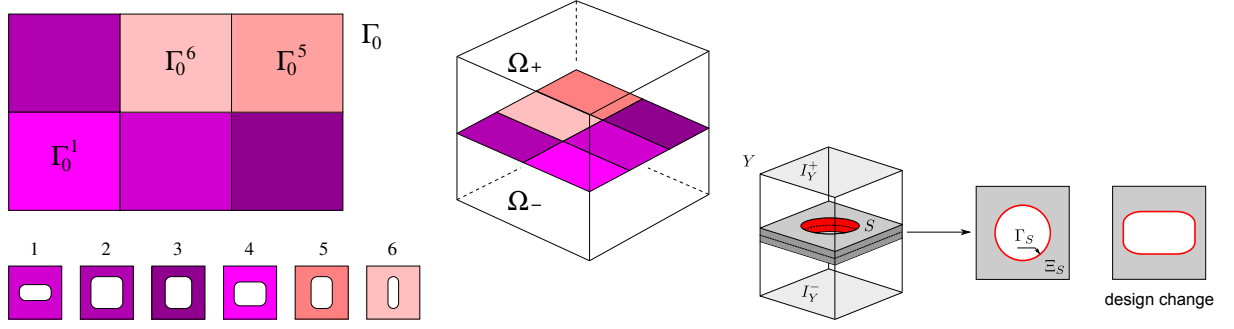


Figure 2: Left: Piecewise periodic perforated plate; six shapes of cylindrical holes. Right: The representative periodic cell Y for homogenization of the vibroacoustic transmission problem. The plate occupies the part S which is generated by the 2D domain Ξ_S . The design-generating curve is $\Gamma_S \subset \partial\Xi_S$.

where $\mathbf{\Pi}^{rs} = (\Pi_i^{rs})$, $\Pi_i^{rs} = y_s \delta_{ri}$ with $i, r, s = 1, 2$. Using solutions of (6) and (7), the homogenized transmission coefficients can be computed:

$$\begin{aligned}
 F &= \int_{I_y^+} \xi - \int_{I_y^-} \xi, \\
 C_k &= \int_{I_y^+} \eta^k - \int_{I_y^-} \eta^k = \int_{\partial S} n_k \xi, \quad k = 3, \\
 T_{kj} &= - \int_{\partial S} \eta^k n_j, \quad k = j = 3, \\
 \bar{\rho}_S &= \int_{\Xi_S} \rho, \\
 C_{ijkl}^H &= c_{\Xi_S} (\bar{\chi}^{kl} + \mathbf{\Pi}^{kl}, \bar{\chi}^{ij} + \mathbf{\Pi}^{ij}), \\
 G_{kl}^H &= \int_{\Xi_S} \gamma \bar{\nabla}_y (\chi^k + y_k) \cdot \bar{\nabla}_y (\chi^l + y_l).
 \end{aligned} \tag{8}$$

3 OPTIMAL DESIGN AND SENSITIVITY ANALYSIS

The design of periodic plate perforations can be controlled by distributed design variables \mathbf{d} which describe the shape of the hole within the representative periodic cell. It is given by the design curve $\Gamma_S := \partial\Xi_S \setminus \partial\Xi$ which determines the simple cylindrical type of perforations, thus the shape of domain Y^* , so that \mathbf{d} influences all the homogenized coefficients presented in Section 2.2. In a more general setting of “nearly-periodic” perforation, the geometry of holes can vary with the global coordinate $x \in \Gamma_0$, so that (6)-(8) are defined locally in a domain Γ_0^k , $k \in \mathcal{K}$ which can be identified with elements of the finite-element partitioning of Γ_0 .

We can now define the *optimal perforation design problem*:

$$\begin{aligned}
 &\min_{\mathbf{d} \in D_{adm}} \Phi(\mathbf{U}) \\
 &\text{subject to: } \mathbf{U} \text{ solves (3),} \\
 &\text{where } F, C_3, T_{33}, \bar{\rho}_S, \mathbf{C}^H, \mathbf{G}^H \text{ are given by local solutions to (6)-(8).}
 \end{aligned} \tag{9}$$

Above D_{adm} is the set of admissible designs, constraining the shape regularity of ∂S and typically some other features, like porosity of the interface. For the “nearly-periodic” perforations, D_{adm} contains some smoothness constraints related to the scale ε_0 .

3.1 Graded perforation and sensitivity analysis

The homogenization method which is employed usually to handle periodic structures, can be applied also in cases, where the structure is only locally periodic. Thus, in general, we can introduce $\Gamma_S(x')$, $x' \in \Gamma_0$ as locally periodic shapes: there exists a nonoverlapping decomposition $\Gamma_0 = \bigcup_{k \in \mathcal{K}} \Gamma_0^k$, $\Gamma_0^k \cap \Gamma_0^l = \emptyset$, if $k \neq l$, such that $\Gamma_S(x') = \Gamma_S^k$ for $x' \in \Gamma_0^k$. Some regularity constraints should be introduced to control the shape variation. Let $\gamma^k : \Gamma_S \mapsto \Gamma_S^k$ be an isomorphism of the reference curve Γ_S on the local curve Γ_S^k and $\mathbf{d}^k = (d_i^k)$ be the design parameters describing the shapes of Γ_S^k , $k \in \mathcal{K}$. Lipschitz continuity $\|\gamma^k - \gamma^l\|_{C^0(\Gamma_S)} \leq C|x^k - x^l|$, where x^k is the barycenter of Γ_0^k , can be expressed by the following constraint on the distributed shape parameters: $|d_i^k - d_i^l| \leq C^{kl}$.

The sensitivity analysis follows the standard flowchart of the adjoint equation technique independently of the number of design variables associated with shapes of Γ_S^k for all local structures k . A special care must be taken when the objective function Φ is real-valued. *Given design*, $\{\mathbf{d}^k\}_{k \in \mathcal{K}} \in D_{adm}$, for a given frequency ω , we proceed by the following steps.

- Compute the state $\mathbf{U} = (p, g, w, \boldsymbol{\theta})$ satisfying the state problem (4)-(5);
- Evaluate the objective function value $\Phi(\mathbf{U})$ and $\delta_U \Phi(\mathbf{U}; \mathbf{V})$.
- Compute the adjoint state $\mathbf{W} = (\tilde{p}, \tilde{g}, \tilde{w}, \tilde{\boldsymbol{\theta}})$ for given state \mathbf{U} and $\delta_U \Phi(\mathbf{U}; \cdot)$, by solving the *adjoint equation* (it splits in two coupled real-valued problem, as will be explained in detail below),

$$2\Re \Psi(\mathbf{V}, \mathbf{W}) = - [\delta_{\Re(\mathbf{U})} \Phi(\mathbf{U}; \mathbf{V}) - i \delta_{\Im(\mathbf{U})} \Phi(\mathbf{U}; \mathbf{V})] \quad \forall \mathbf{V} \in \mathcal{U}_0; \quad (10)$$

- Compute the *shape sensitivity* $(\delta_{sh} F, \delta_{sh} C_3, \delta_{sh} T_{33}, \delta_{sh} \bar{\rho}_S, \delta_{sh} \mathbf{C}^H, \delta_{sh} \mathbf{G}^H)$ of the homogenized coefficients w.r.t. the distributed parameters \mathbf{d}^k , $k \in \mathcal{K}$; see [3] for details. For simplicity, we assume the shape derivative of Φ vanishes, i.e. $\delta_{sh} \Phi = 0$.
- Evaluate the total variation using the *final sensitivity formula*:

$$\begin{aligned} \delta \Phi(\mathbf{U}) := & 2\Re \left\{ \omega^2 [\partial_{C_3} \mathcal{C}(w, \tilde{g}) + \partial_{C_3} \mathcal{C}(\tilde{w}, g)] \circ \delta_{sh} C_3 - \omega^2 \partial_F \mathcal{F}(g, \tilde{g}) \circ \delta_{sh} F \right. \\ & - \omega^2 \left[\partial_{(\bar{\rho}_S, T_{33})} \mathcal{N}(w, \tilde{w}) \circ (\delta_{sh} \bar{\rho}_S, \delta_{sh} T_{33}) + \partial_{\bar{\rho}_S} \mathcal{M}(\boldsymbol{\theta}, \tilde{\boldsymbol{\theta}}) \circ \delta_{sh} \bar{\rho}_S \right] \\ & \left. + \partial_{\mathbf{C}^H} \mathcal{E}(\bar{\nabla}^S \boldsymbol{\theta}, \bar{\nabla}^S \tilde{\boldsymbol{\theta}}) \circ \delta \mathbf{C}^H + \partial_{\mathbf{G}^H} \mathcal{G}(\bar{\nabla} w - \boldsymbol{\theta}, \bar{\nabla} \tilde{w} - \tilde{\boldsymbol{\theta}}) \circ \delta_{sh} \mathbf{G}^H \right\}. \end{aligned} \quad (11)$$

To compute the shape sensitivity (above denoted by δ_{sh}) of the homogenized coefficients, we use the material derivative as the standard tool see [2]; the particular formulae can be found in [3].

3.2 Computing the adjoint state

As the objective function is real-valued and, thus, admits the real sensitivity only, whereas the state problem leads to complex valued solutions, some care must be devoted to compute the adjoint states $(\hat{p}, \hat{g}, \hat{w}, \hat{\boldsymbol{\theta}})$ involved in (11). In fact, (10) splits into two systems which, however, are coupled. For nonvanishing real parts $(q_r, \psi_r, z_r, \boldsymbol{\vartheta}_r)$ of the test functions, one obtains the set of equations displayed in Tab. 1. Similarly, for nonvanishing imaginary parts $(q_i, \psi_i, z_i, \boldsymbol{\vartheta}_i)$, the set of equations is displayed in Tab. 2.

$c^2 (\nabla q_r, \cdot \nabla \hat{p}_r)_\Omega$ $-\omega^2 (q_r, \hat{p}_r)_\Omega$ $-\omega c \langle q_r, \hat{p}_r \rangle_{\Gamma_{\text{in-out}}}$	$+\varepsilon_0^{-1} \omega \langle \hat{g}_i, [q_r]_-^+ \rangle_{\Gamma_0}$		$= -\partial_p \Phi(\mathbf{U}; q_r),$
$-c^2 \omega \langle \psi_r, [\hat{p}_r]_-^+ \rangle_{\Gamma_0}$	$-\omega^2 \mathcal{F}(\psi_r, \hat{g}_r)$	$+\omega^2 \mathcal{C}(\psi_r, \hat{w}_r)$	$= -\partial_g \Phi(\mathbf{U}; \psi_r),$
	$\omega^2 \mathcal{C}(z_r, \hat{g}_r)$	$+\mathcal{G}(\bar{\nabla} z_r, \bar{\nabla} \hat{w}_r)$ $-\omega^2 \mathcal{N}(z_r, \hat{w}_r)$	$-\mathcal{G}(\bar{\nabla} z_r, \hat{\theta}_r) = -\partial_w \Phi(\mathbf{U}; z_r),$
		$-\mathcal{G}(\vartheta_r, \bar{\nabla} \hat{w}_r)$	$+\mathcal{G}(\vartheta_r, \hat{\theta}_r)$ $+\mathcal{E}(\bar{\nabla}^S \vartheta_r, \bar{\nabla}^S \hat{\theta}_r)$ $-\omega^2 \mathcal{M}(\vartheta_r, \hat{\theta}_r) = -\partial_\theta \Phi(\mathbf{U}; \vartheta_r),$

 Table 1: Adjoint equation, to hold for all $(q_r, \psi_r, z_r, \vartheta_r) \in \mathcal{U}_0$

$c^2 (\nabla q_i, \cdot \nabla \hat{p}_i)_\Omega$ $-\omega^2 (q_i, \hat{p}_i)_\Omega$ $+\omega c \langle q_i, \hat{p}_i \rangle_{\Gamma_{\text{in-out}}}$	$-\varepsilon_0^{-1} \omega \langle \hat{g}_r, [q_i]_-^+ \rangle_{\Gamma_0}$		$= -\partial_p \Phi(\mathbf{U}; q_i)$
$c^2 \omega \langle \psi_i, [\hat{p}_i]_-^+ \rangle_{\Gamma_0}$	$-\omega^2 \mathcal{F}(\psi_i, \hat{g}_i)$	$+\omega^2 \mathcal{C}(\psi_i, \hat{w}_i)$	$= -\partial_g \Phi(\mathbf{U}; \psi_i),$
	$\omega^2 \mathcal{C}(z_i, \hat{g}_i)$	$+\mathcal{G}(\bar{\nabla} z_i, \bar{\nabla} \hat{w}_i)$ $-\omega^2 \mathcal{N}(z_i, \hat{w}_i)$	$-\mathcal{G}(\bar{\nabla} z_i, \hat{\theta}_i) = -\partial_w \Phi(\mathbf{U}; z_i),$
		$-\mathcal{G}(\vartheta_i, \bar{\nabla} \hat{w}_i)$	$+\mathcal{G}(\vartheta_i, \hat{\theta}_i)$ $+\mathcal{E}(\bar{\nabla}^S \vartheta_i, \bar{\nabla}^S \hat{\theta}_i)$ $-\omega^2 \mathcal{M}(\vartheta_i, \hat{\theta}_i) = -\partial_\theta \Phi(\mathbf{U}; \vartheta_i),$

 Table 2: Adjoint equation, to hold for all $(q_i, \psi_i, z_i, \vartheta_i) \in \mathcal{U}_0$

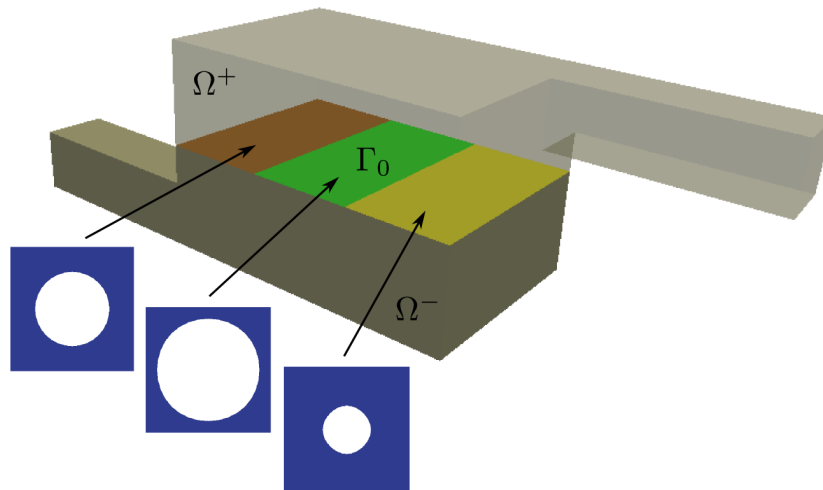


Figure 3: Geometry of a waveguide with piecewise periodic design of the perforated plate.

4 CONCLUSIONS

We developed a homogenized model of the simply perforated plate to serve a vibro-acoustic transmission expressed in terms of the transversal acoustic velocity which couples traces of the discontinuous acoustic pressure field. These transmission conditions introduce also three other “internal variables”, the deflection and two rotations associated with the Reissner–Mindlin type of the plate. The model can be extended easily for multiple plates which are used to enhance the acoustic absorption, cf. [10].

We consider optimal perforation design problems. The sensitivity analysis based on the shape derivative of the perforation geometry and the adjoint equation technique was developed which enables to compute efficiently gradients of general real-valued objective functions, such as two-point transmission loss, or other functionals involving all the “macroscopic” fields, including the plate deflections. The shape sensitivity was described in more details in [3], whereas in this paper we focused on the adjoint technique application. Numerical tests will be subject of a forthcoming publication. For illustration, we computed acoustic pressure field in a waveguide depicted in Fig. 3.2. The plate consists of three parts with different shape of the perforations. To design variables introduced as the control points of the spline-parametrized volume, see Fig. 4, modify the computational cells Y and Ξ_S related to the acoustic and plate local problems reported in Section 3. In Tab. 3 the homogenized coefficients are listed for two designs of the perforation. The global response in waveguide is depicted in Fig. 5. All computations are performed using our in-house developed FEM code SfePy, <http://sfepy.org>.

Acknowledgments The research of was supported by the European Regional Development Fund (ERDF), project “NTIS – New Technologies for Information Society”, European Centre of Excellence, CZ.1.05/1.1.00/02.0090, and in part by the Czech Scientific Foundation project GACR P101/12/2315.

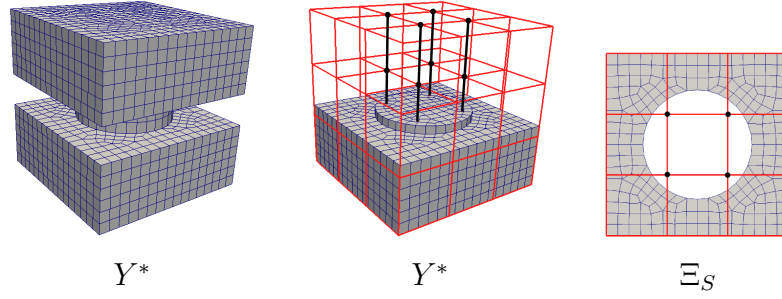


Figure 4: The FE mesh of the computational cell Y^* (left), embedded in the transmission layer and its 3D B-spline parameterization (middle). The computational cell Ξ_S and its 2D B-spline parametrization describing the plate structure (right).

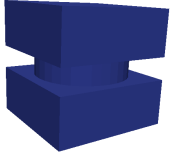

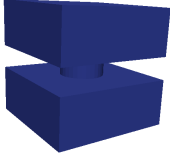

	$F = -1.354$ $C_3 = -0.354$ $T_{33} = 0.260$		$\mathbf{C}^H = \begin{bmatrix} 2.370 & 0.494 & 0.0 \\ 0.494 & 2.370 & 0.0 \\ 0.0 & 0.0 & 0.248 \end{bmatrix} \cdot 10^{10}$ $\mathbf{G}^H = \begin{bmatrix} 2.419 & 0.0 \\ 0.0 & 2.419 \end{bmatrix} \cdot 10^{10}$
	$F = -4.037$ $C_3 = -3.037$ $T_{33} = 2.859$		$\mathbf{C}^H = \begin{bmatrix} 7.670 & 3.592 & 0.0 \\ 3.592 & 7.670 & 0.0 \\ 0.0 & 0.0 & 1.899 \end{bmatrix} \cdot 10^{10}$ $\mathbf{G}^H = \begin{bmatrix} 6.403 & 0.0 \\ 0.0 & 6.403 \end{bmatrix} \cdot 10^{10}$

Table 3: Coefficients of the homogenized transmission condition model for two perforations.

REFERENCES

- [1] D. Cioranescu, A. Damlamian and G. Griso, The periodic unfolding method in homogenization, *SIAM Journal on Mathematical Analysis*, Vol. **40**, 1585-1620, 2008.
- [2] J. Haslinger and P. Neittaanmäki, *Finite Element Approximation for Optimal Shape, Material and Topology Design*, 2nd ed. J. Wiley & Sons, Chichester, U.K., 1996.
- [3] E. Rohan and V. Lukes, Sensitivity analysis for optimal design of perforated plates in vibro-acoustics: homogenization approach. In *Proceedings of ISMA 2012 - USD 2012*. Leuven: KU Leuven, 4201-4214, 2012. ISBN: 978-907-380-289-6
- [4] E. Rohan and B. Miara, *Sensitivity analysis of acoustic wave propagation in strongly heterogeneous piezoelectric composite*, in: *Topics on Mathematics for Smart Systems*, World Sci. Publ., 139-207, 2006.
- [5] E. Rohan and B. Miara, Homogenization and shape sensitivity of microstructures for design of piezoelectric bio-materials, *Mechanics of Advanced Materials and Structures* **13**, 473-485, 2006.
- [6] E. Rohan and V. Lukeš, Homogenization of the acoustic transmission through perforated layer, *J. of Comput. and Appl. Math.*, **234**, 1876–1885, 2010.
- [7] E. Rohan and V. Lukeš, *Homogenized perforated interface in acoustic wave propagation – modeling and optimization*, in J. Náprstek et al, editors, *Proc. of the 10th International*

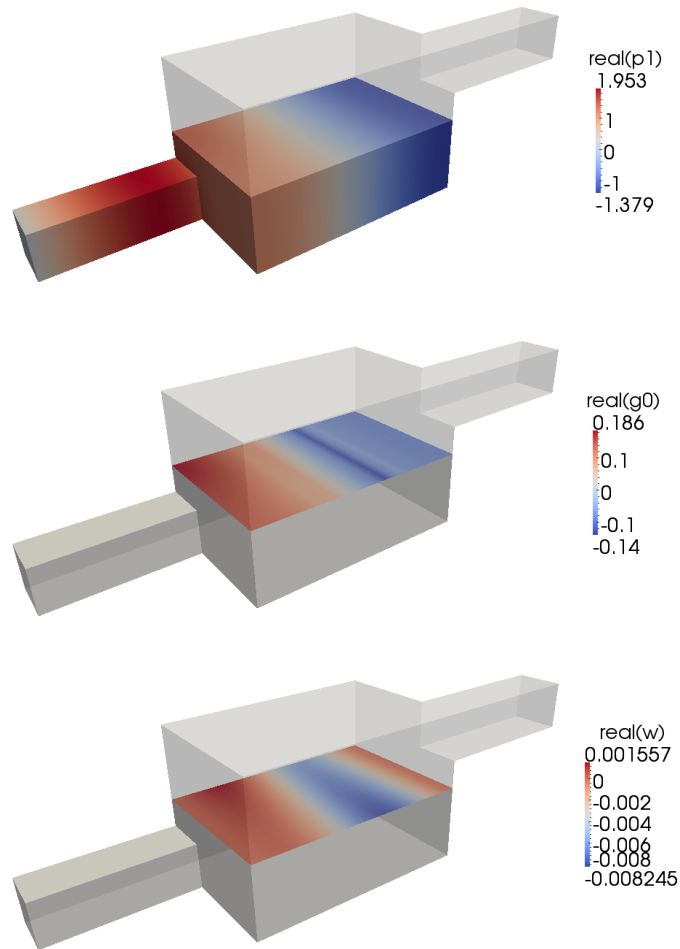


Figure 5: Acoustic pressure field $\Re p$ in Ω^- (the real part), transversal acoustic velocity $\Re g_0$ on Γ_0 and the plate deflection $\Re w$. The perforation considered as in Fig. 3.2.

Conference on Vibration Problems, ICOVP 2011, Springer Proceedings in Physics, **139**, 321-327, 2011.

- [8] E. Rohan, V. Lukeš and B. Miara, Homogenization of the vibro–acoustic transmission on perforated Reissner-Mindlin plate, *Proceedings of The 10th International Conference on Mathematical and Numerical Aspects of Waves (Waves 2011)*, Vancouver, 2011, <http://www.sfu.ca/WAVES/proceedings/>
- [9] E. Rohan and B. Miara, Band gaps and vibration of strongly heterogeneous Reissner-Mindlin elastic plates, *Comptes Rendus Mathematique*, **349**, 777-781, 2011.
- [10] Sung S. Jung et al. Sound absorption of micro-perforated panel. *Journal of the Korean Physical Society*, **50**, 1044–1051, 2007.